Eur. Phys. J. C 56, 221–229 (2008)
DOI 10.1140/epjc/s10052-008-0651-1

THE EUROPEAN PHYSICAL JOURNAL C

Regular Article – Theoretical Physics

Quark sea structure functions of the nucleon in a statistical model

L.A. Trevisan[1], C. Mirez[2], T. Frederico[3], L. Tomio[2,a]

[1] Departamento de Matemática e Estatística, Universidade Estadual de Ponta Grossa, 84010-790, Ponta Grossa, PR, Brazil
[2] Instituto de Física Teórica, Universidade Estadual Paulista, Rua Pamplona, 145, 01405-900, São Paulo, SP, Brazil
[3] Departamento de Física, Instituto Tecnológico de Aeronáutica, CTA, 12228-900, São José dos Campos, SP, Brazil

Received: 12 May 2008 / Revised version: 21 May 2008 /
Published online: 2 July 2008 –

Abstract. Within a statistical model of linear confined quarks we obtain the flavor asymmetry and corresponding structure function of the nucleon. The model parameters are fixed by the experimental available data. The temperature parameter is adjusted by the Gottfried sum rule violation and the chemical potentials by the corresponding up (u) and down (d) quark normalizations in the nucleon. The light antiquark and quark distributions in the proton, given by $\overline{d}/\overline{u}$, d/u and $\overline{d}-\overline{u}$, as well as the neutron to proton ratio of the structure functions, extracted from the experimental data, are well fitted by the model. As the quark-confining strengths should be flavor dependent, a mechanism is introduced in the model to adjust the corresponding distribution, in order to improve the comparison obtained for the sea-quark asymmetries in the nucleon with the available experimental analysis.

PACS. 11.30.Hv; 14.20.Dh; 12.39.Ki; 12.40.Ee; 11.55.Hx

1 Introduction

The analysis of the available experimental data [1, 2] for the sea-quark distributions has shown that there is not a simple model explanation on the light antiquark distribution, $\bar{d}/\bar{u}$, in the sea of the nucleon. For instance, if we are considering only perturbative QCD and gluon splitting processes, the violation of the Gottfried sum rule (GSR) [3] is not reproduced, as the ratio $\bar{d}/\bar{u}$ becomes equal to one, due to the equal probabilities of gluon splittings in $d\bar{d}$ or $u\bar{u}$ pairs. In a model with a virtual pion [4–11] the GSR can be reproduced, but there is a large discrepancy from theoretical and experimental curves for large x. (For some reviews, see [12, 13]). Following an idea first presented by Field and Feynman [14], it was shown that the Pauli exclusion principle can be considered in statistical models to obtain different quantities of $\bar{u}$ and $\bar{d}$ in the nucleon sea [15–19]. In this respect, the statistical quark model of [19] was proved to be useful to reproduce some aspects of the flavor structure of the nucleon, as the strangeness content of the nucleon, and the difference between the structure functions of the proton and neutron.

On the other hand, the ratio d/u also contains important information about the flavor structure of the proton. In particular, its asymptotic behavior at large x may indicate the mechanism responsible for the $\mathrm{SU}(2)_{\mathrm{spin}} \times \mathrm{SU}(2)_{\mathrm{flavor}}$ symmetry breaking. The distribution of u and d valence quarks in the proton can be determined from any two observables containing linear combinations of the u and d quarks, which are usually taken to be the proton and neutron structure function, F_2^p and F_2^n. While F_2^p is quite well constrained for light-cone momentum fractions $x = Q^2/2M\nu \lesssim 0.8$, F_2^n is usually extracted from data on the deuteron. However, beyond $x \sim 0.5$, the large nuclear corrections may result in uncertainties of up to $\sim 50\%$ in the neutron to proton structure function ratio, F_2^n/F_2^p [20–23]. Previous analyses [24] have used inclusive deep-inelastic scattering (DIS) data on the proton and deuteron targets to obtain the neutron to proton structure function ratio, from which d/u can be extracted at large x according to

$$\frac{F_2^n}{F_2^p} = \frac{4d+u}{4u+d}\,, \quad \frac{d}{u} = \frac{4F_2^n - F_2^p}{4F_2^p - F_2^n}\,, \quad x \to 1\,. \tag{1}$$

Several alternatives to obtain an independent linear combination of u and d quark distributions have been suggested which could minimize or avoid the problem of nuclear corrections [25–28]. With respect to DIS, it is known that the d quark distribution is softer than the u quark one, with F_2^n/F_2^p deviating at large x from the SU(6) expectation. Different non-perturbative mechanisms that break SU(6) symmetry have been suggested [29–32] to fit the data in the region of x where F_2^n/F_2^p can be reliably extracted. Theoretical predictions and experimental data of these quantities are, respectively, given in [33–38] and [39, 40].

[a] e-mail: tomio@ift.unesp.br

In the present work, we follow the phenomenological statistical model presented in [19], with linear confined quarks, to obtain the flavor asymmetry in the sea of the nucleon (given by $\bar{u}/\bar{d}$, u/d and $\bar{d}-\bar{u}$) and the corresponding ratio between the proton and neutron structure functions. The model is parameterized by the experimental available data, with a temperature parameter given by the GSR violation and the chemical potentials by the net number of u and d quarks in the nucleon. Two different chemical potentials are required to describe the nucleon; one fixes the net number of u quarks and the other the net number of d quarks. The approach given in [19] was inspired by the models studied in [17, 18]. However, instead of assuming continuum levels for the quark energies, as in [17, 18], quark levels given by a Dirac confining potential [41] were considered to generate the single-particle spectrum, where the quarks obey the Fermi statistics. The strength of the confining potential, for each quark flavor λ_q, is fitted through the hadron masses, where we assume $\lambda_u = \lambda_d \equiv \lambda$ and $m_u = m_d = 0$.

The main motivation of using the present model is to deal directly with the fundamental degrees of freedom of QCD. Having insight in the model parametrization one accesses qualitative information on the quark content of the nucleon wave function. The statistical quark model of the nucleon sea averages the Fock state content of the decomposition of the wave function with a statistical description capable to implement correctly the isospin and Pauli principle. The correct antisymmetrization within each Fock component is implemented at the level of single particles by the Fermi–Dirac distributions. Thus, the chemical potential and temperature give a simple parametrization of quarks and antiquarks probabilities in the Fock components of the wave function. A strong test of the model is given by the possibility to obtain, in principle, the experimental observables related to heavier quark content of the nucleon sea, as the strange quark content of the nucleon which is well reproduced by the model [19].

It is worthwhile to point out that the question of developing a quark model with confining potential incorporating x-dependence in the valence quarks distribution functions is not an easy task, as observed in [42], in the context of the *chiral bag model*, in [43, 44], in a chiral quark soliton model, and, more recently, in [45], in a *chiral constituent quark model with configuration mixing*. One recent approach to the incorporation of the x-dependence in the quark distribution functions was suggested in [46] from assumptions regarding the non-perturbative properties of the hadron wave function. Instead, in the present statistical quark model, the x-dependence of the probability functions and related observables are derived from a dynamical input, i.e., the relativistic quark confining potential. The momentum representation of the quark eigenstates of the Dirac Hamiltonian is rewritten in terms of the light-cone momenta allowing one to extract the x-dependence of the quark amplitudes. The key point that made this transformation simple is the single-particle nature of the model.

The next sections are organized as follows: in Sect. 2, we make a brief description of the statistical quark model developed in [19]. In Sect. 3, the model is improved with different effects affecting the u and d quark distributions. By considering instanton effects to probably be responsible for different u and d mean-field interactions in the nucleon, which affect the corresponding distribution over the Bjorken scale x, in the first subsection we incorporate this effect in the model as an effective light-quark mass shift. In the following two subsections we discuss the contribution from gluonic splitting and pionic processes in the nucleon structure function. In Sect. 4, the main results of our model are presented. Finally, our concluding remarks are given in Sect. 5.

2 Statistical quark model with confining potential

In the present statistical quark model all individual quarks of the system, valence and sea quarks, are confined by a central effective interaction, with strength λ and equal expressions for the scalar and vector components, given by [41]

$$V(r) = (1+\beta)\frac{\lambda r}{2}\,. \tag{2}$$

So, the energy levels of the confined quark are obtained from the stationary Dirac equation,

$$[\boldsymbol{\alpha}\mathbf{p} + \beta m + V(r)]\psi_i(\mathbf{r}) = \varepsilon_i \psi_i(\mathbf{r})\,. \tag{3}$$

In (2) and (3), β and $\boldsymbol{\alpha}$ are the usual 4×4 Dirac matrices, which can be written in terms of the 2×2 Pauli matrices. With $\psi_i(\mathbf{r})$ given by [41]

$$\psi_i(\mathbf{r}) = \begin{pmatrix} 1 \\ \boldsymbol{\sigma}\mathbf{p}/(m+\varepsilon_i) \end{pmatrix} \varphi_i(\mathbf{r})\,, \tag{4}$$

the final coupled equations will be reduced to a single second order differential equation,

$$\left[\mathbf{p}^2 + (m+\varepsilon_i)(m+\lambda r - \varepsilon_i)\right]\varphi_i = 0\,. \tag{5}$$

This equation is solved for the radial part, after a partial wave expansion. For s-wave ($l=0$), where $j^p = (\frac{1}{2})^+$, the radial part of φ_i is related to the Airy function (Ai):

$$\varphi_i(r) = \sqrt{\frac{K_i}{4\pi}}\frac{\mathrm{Ai}(K_i r + a_i)}{r\left[\frac{\mathrm{d}\,\mathrm{Ai}(x)}{\mathrm{d}x}\right]\Big|_{x=a_i}}\,, \tag{6}$$

where a_i is the corresponding ith root of Ai(x), $K_i \equiv \sqrt[3]{\lambda(m+\varepsilon_i)}$, m is the current quark mass, and the ε_i are the energy levels,

$$\varepsilon_i = m - \frac{\lambda}{K_i} a_i\,. \tag{7}$$

For the u and d quarks with $m=0$, the energies are given by

$$\varepsilon_i = \sqrt{\lambda}(-a_i)^{\frac{3}{4}}\,. \tag{8}$$

We use equal strengths for the u and d quarks. The sum of the first energy level of these quarks results in the Δ mass. For a system constituted by confined quarks, this will be corrected for by the nucleon mass by introducing instanton interactions, which reduce the mass value.

Next, we consider the Fermi–Dirac distributions of the quarks in the present statistical quark model. The probability density for a quark system, with energy levels ε_i and temperature T, is given by

$$\rho_q(\mathbf{r}) = \sum_i g_i \psi_i^\dagger(\mathbf{r})\psi_i(\mathbf{r}) \frac{1}{1+\exp\left(\frac{\varepsilon_i-\mu_q}{T}\right)} . \tag{9}$$

With the appropriate chemical potential μ_q $(= -\mu_{\bar{q}})$ and with the normalized wave function, we can fit the quark flavor number q $(\equiv u, d, s, \bar{u}, \bar{d}, \bar{s})$ in the nucleon and the violation of GSR. g_i gives the level degeneracy and $|\psi_i(\mathbf{r})|^2$ the density probability for each state, normalized to 1,

$$\int \psi_i^\dagger(\mathbf{r})\psi_i(\mathbf{r})\,\mathrm{d}^3r = 1 . \tag{10}$$

In the present work we consider only the light quarks, u and d, with the corresponding current quark masses given by $m_u = m_d = 0$. The energies are taken to be equal for the u and d quarks, obtained by using a confining potential model in the Dirac equation. With the above, we obtain the following normalization for the proton (neutron):

$$\begin{aligned} &\int [\rho_q(\mathbf{r}) - \bar{\rho}_q(\mathbf{r})]\,\mathrm{d}^3r \\ &= \sum_i g_i \left[\frac{1}{1+\exp\left(\frac{\varepsilon_i-\mu_q}{T}\right)} - \frac{1}{1+\exp\left(\frac{\varepsilon_i+\mu_q}{T}\right)}\right] \\ &= \begin{cases} 1 & \text{for } q = d(u) \\ 2 & \text{for } q = u(d) \end{cases} \end{aligned} \tag{11}$$

The units we are using are such that the Boltzmann constant k, $\hbar$, and c are all set to 1. The averaged masses (also referred to as "thermal masses" due to their dependence on the parameter T) for the proton (M_p) and neutron (M_n) are given in terms of the corresponding energy levels, as follows:

$$\left.\begin{aligned} M_p &= 2M_u + M_d \\ M_n &= 2M_d + M_u \end{aligned}\right\} = \sum_{q=u,d} \sum_i g_i \left[\frac{\varepsilon_i}{1+\exp\left(\frac{\varepsilon_i-\mu_q}{T}\right)} + \frac{\varepsilon_i}{1+\exp\left(\frac{\varepsilon_i+\mu_q}{T}\right)}\right] . \tag{12}$$

In order to calculate the nucleon structure function, we write the wave function in momentum space, taking the Fourier transform

$$\Phi_i(\mathbf{p}) = \frac{1}{(2\pi)^{3/2}} \int \exp(-\mathrm{i}\mathbf{pr})\psi_i(\mathbf{r})\,\mathrm{d}^3r . \tag{13}$$

Using the null plane variables,

$$\begin{aligned} p^+ &= xP^+ , \quad P^+ = M_N \quad (N \equiv n, p) \\ p_z &= p^+ - \varepsilon_i = M_N\left(x - \frac{\varepsilon_i}{M_N}\right) , \end{aligned} \tag{14}$$

where x is the momentum fraction of the nucleon carried by the quark, M_N is the nucleon thermal mass at a given temperature T, we redefine the wave function (13) as

$$\Phi_i(\mathbf{p}) \equiv \Phi_i(x, \mathbf{p}_\perp) . \tag{15}$$

By using (9)–(15), we obtain the quark structure function for each flavor q:

$$q_T(x) = \sum_i \int \mathrm{d}^2p_\perp \frac{\Phi_i^\dagger \Phi_i}{1+\exp\left(\frac{\varepsilon_i-\mu_q}{T}\right)} , \tag{16}$$

where

$$\Phi_i \equiv \Phi_i\left(M_N\left(x - \frac{\varepsilon_i}{M_N}\right), \mathbf{p}_\perp\right) . \tag{17}$$

$q_T(x)$ describes the probability that a quark with flavor q has a fraction x of the total momentum of the nucleon, assuming a temperature T. For the corresponding antiquark distribution, $\bar{q}_T(x)$, we have to replace μ_q by $-\mu_q$ in (16).

In the model, we consider the result given by the NMC Collaboration [47, 48],

$$S_\mathrm{G} \equiv \int_0^1 \frac{\mathrm{d}x}{x}\left(F_2^{\mu p}(x) - F_2^{\mu n}(x)\right) = 0.235 \pm 0.026 , \tag{18}$$

implying that the violation of the GSR is given by

$$I_\mathrm{GSR} \equiv \frac{1}{2} - \frac{3}{2}S_\mathrm{G} = \int_0^1 \left(\bar{d}(x) - \bar{u}(x)\right)\,\mathrm{d}x = 0.148 \pm 0.039 . \tag{19}$$

The statistical model of [19] reproduces this result with a temperature parameter T adjusted to 108 MeV, with the chemical potentials $\mu_u = 135$ MeV and $\mu_d = 78$ MeV. Actually, from the analysis of the E866 experiments [1, 2], the value for the violation of the GSR is $I_\mathrm{GSR} = 0.100 \pm 0.018$. This implies a readjustment of the parameters of the same statistical model, such that $T \approx 103$ MeV, $\mu_u \approx 147$ MeV, and $\mu_d \approx 88$ MeV. The total quantity of the $\bar{d}$ is recalculated to be $\bar{d} = 0.24$ and $\bar{u} = 0.14$. With such results, the ratio $\bar{d}/\bar{u}$ is constant,

$$\frac{\bar{d}_T}{\bar{u}_T} = 1.71 , \tag{20}$$

while the corresponding experimental data present a strong x-dependence (see Fig. 3).

2.1 Strangeness content of the nucleon

The strangeness content of the nucleon was also well reproduced by the model given in [19]. This observable is important for verifying the consistency of the model when describing the hadron in terms of its contents. Recently, the strangeness of the nucleon was studied in model parametrizations [45, 49] and also by a statistical quark model [50]. As shown in [19], the results for the strangeness are not too much sensitive to the model parametrization once the GSR violation and the normalizations of the valence quarks inside the nucleon are fixed.

In this case, the relevant observables are given by [51]

$$\eta = \frac{2\int_0^1 xs(x)\,\mathrm{d}x}{\int_0^1 x(u(x)+d(x))\,\mathrm{d}x}, \quad \kappa = \frac{2\int_0^1 xs(x)\,\mathrm{d}x}{\int_0^1 x(\bar{u}(x)+\bar{d}(x))\,\mathrm{d}x}. \tag{21}$$

κ represents the ratio between the strange and non-strange quark of the sea. With η/κ we obtain the ratio between the non-strange antiquarks and quarks in the nucleon:

$$\frac{\eta}{\kappa} = \frac{\int_0^1 (\bar{u}(x)+\bar{d}(x))x\,\mathrm{d}x}{\int_0^1 (u(x)+d(x))x\,\mathrm{d}x}. \tag{22}$$

From [19, Table V] we observe that, when the temperature is about 108 MeV, by fitting the GSR violation to $I_{\mathrm{GSR}} = -0.14$, the numerical results for η and κ are, respectively, 0.085 and 0.536, in good agreement with the experimental data [$\eta = 0.099$, $\kappa = 0.477$]. The experimental data for the strangeness were obtained from [52].

Next, within the statistical quark model approach [19], after we have adjusted the GSR violation with a temperature parameter, we implement an analysis to fit the experimental data for the ratios of the quark distributions inside the proton, given by $\bar{d}/\bar{u}$ and d/u. The model also provides the corresponding sea-quark difference $\bar{d}-\bar{u}$ and the ratio between the neutron to proton structure functions, F_2^n/F_2^p.

3 Effective quark mass shift, gluonic and pionic effects

3.1 Effective light-quark mass shift

The difference between the interactions of the u and d quarks in the nucleon is supposed to come from instanton contributions, which are flavor-spin dependent [53]. Each quark interacts with another, of opposite spin and different flavors. In the present approach, we use the quark distributions given in Sect. 2. To consider the instanton contribution in an effective way, we note that d-quarks in the proton have a more attractive channel, with the energy lower than that of the u-quarks. In this model, as the initial confining potential is the same, there is no difference between the quark energies. It follows that the ratios d/u and $\bar{d}/\bar{u}$ are constant. Once given any quark distribution $q(x)$, a simple mathematical way to implement the above considerations is to shift the distributions over the x scale, in such a way that $u(x)$ and $d(x)$ (and the corresponding antiparticle) distributions have their respective maxima at different x positions. Note that working with both particle and antiparticle distributions one can obtain at once all ratios between the structure functions. The physical meaning behind the displacement is that the effective potential for the u and d quarks should be different, and also for their antiparticles. In the Fock space, a $|uud\bar{u}u\rangle$ state is more energetic than a state $|uud\bar{d}d\rangle$.

The shift of the x scale can be done for any probability distribution. In the following, to verify the effect of such a shift, we choose the simplest distribution, given by the Dirac delta function (see, for example, [54, Chapt. 9]):

$$q(x) = \delta\left(\frac{M_q}{M_n} - x\right), \tag{23}$$

where M_q is a quark mass and M_n is the total mass of the nucleon. The distribution above is valid for u and d quarks in the case that they are considered to have equal masses. When $M_q \neq M_u \neq M_d$, the new distributions for $u(x)$ and $d(x)$ are shifted in relation to $q(x)$, such that $u(x)$ can be

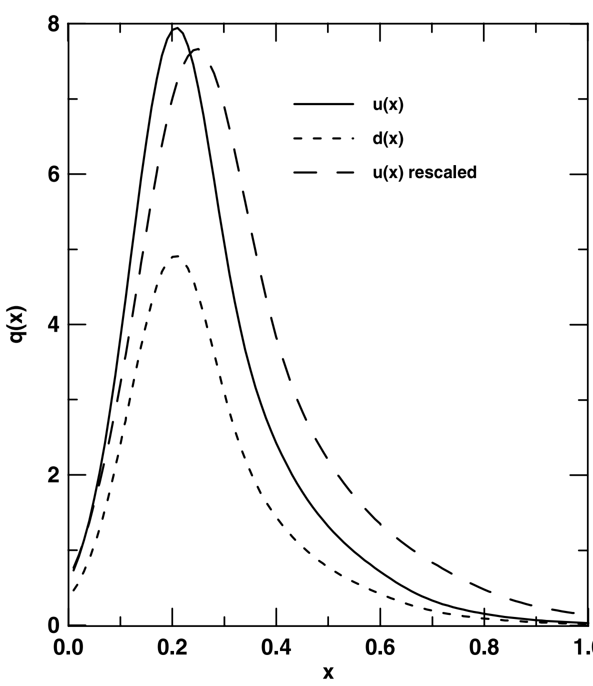

Fig. 1. The u and d quark structure functions for the proton in the statistical quark model are shown as functions of the Bjorken momentum scale x. The results for the d-quark distribution are presented with the *short-dashed line*. For the u-quark distribution, we show two *plots*: one of the *plots* (*solid line*) assuming equal masses ($M_u = M_d \equiv M_q$), the other (*long-dashed line*), assuming $M_u/M_q = 1.25$, having the maximum shifted to the right-hand side

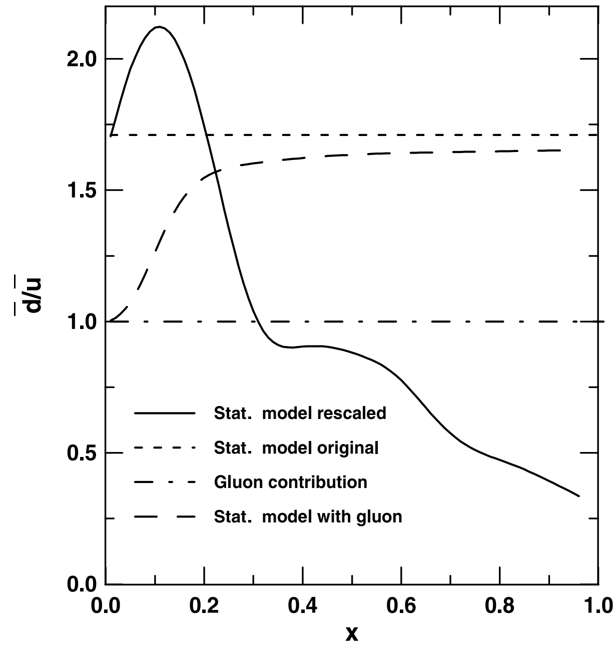

Fig. 2. The amount of contributions to the antiquark ratio $\bar{d}/\bar{u}$ are shown as functions of x. The contributions are from the original statistical model (*dotted line*); gluonic (*dot-dashed line*); and the statistical model plus gluonic contributions (*dashed line*). Considering only the original statistical model, we also show the effect of mass rescaling with the *solid line*

written as

$$u(x) = \delta\left(\frac{M_u}{M_q}\frac{M_q}{M_n} - x\right)$$
$$= \frac{M_q}{M_u}\delta\left(\frac{M_q}{M_n} - \frac{M_q}{M_u}x\right) = \frac{M_q}{M_u}q\left(\frac{M_q}{M_u}x\right). \quad (24)$$

So, when $\left(\frac{M_u}{M_q}\right) > 1$, the rescaled function will have the maximum shifted to the right of the original function, as shown in Fig. 1. For a reasonable fit of the observables, in the present work we consider $M_u/M_q \approx 1.25$, where for the proton $M_q \equiv M_d$.

In Fig. 2, we show the different contributions to the antiquark ratio $\bar{d}/\bar{u}$. The effect of the mass rescaling is shown by the solid line. As shown, the ratios $\bar{d}/\bar{u}$ and d/u are sensitive to the mass displacement, which can be related to the effective quark confining strengths. This effect is being used to improve the overall fitting of the sea-quark ratios and neutron to proton structure function ratios.

3.2 Gluon splitting process

In this subsection we consider the perturbative QCD process of gluon emission by quarks, being splitted in quark–antiquark pairs. Such gluon splitting is a well studied process [54]. There are equal chances to originate $d\bar{d}$ or $u\bar{u}$ pairs from any quark. For the quark source of the perturbative gluons, we can use the sum of quark–antiquark probabilities given in the statistical model by the function

$$f_T(x) = u_T(x) + \bar{u}_T(x) + d_T(x) + \bar{d}_T(x)\,. \quad (25)$$

The probability of particle–antiparticle pairs from gluon emissions is given by the Gribov–Lipatov–Altarelli–Parisi equation [55]. We first consider gluon creation from the original quark distribution and after the splitting of the gluons. An equal number of each flavor of light quarks is created [54, 56, 57].

The joint probability density to obtain a quark coming from the subsequent decays $q \to q+g$ and $g \to q+\bar{q}$ at some fixed low Q_v^2 is given by

$$q_g(x) = \frac{N\alpha_s^2\left(Q_v^2\right)}{(2\pi)^2}\int_x^1 \mathrm{d}y \frac{P_{qg}\left(\frac{x}{y}\right)}{y}\int_y^1 \frac{\mathrm{d}z}{z}P_{gq}\left(\frac{y}{z}\right) f_T(z)\,, \quad (26)$$

where we use the index g to indicate that the quarks are generated by gluon splitting processes, given by the functions P_{qg} and P_{gq} [54]:

$$P_{gq}(z) = \frac{4}{3}\frac{1+(1-z)^2}{z}\,, \quad P_{qg}(z) = \frac{1}{2}\left(1-2z+2z^2\right). \quad (27)$$

The probability given in (26) is the same for the quark and antiquark, such that $q_g(x) = \bar{q}_g(x)$. Hence, the model has two sea-quark components, the temperature-dependent component, which gives the violation of GSR, and a component that comes from QCD perturbative processes, equal for all quarks. This second component, when dominating, makes $\bar{d}/\bar{u} \simeq 1$, as shown by

$$\frac{\bar{d}(x)}{\bar{u}(x)} = \frac{\bar{d}_T(x) + q_g(x)}{\bar{u}_T(x) + q_g(x)}\,. \quad (28)$$

Note that with only the considerations of Sects. 2 and gluonic effects, the ratio $\bar{d}/\bar{u}$ will be constant. This occurs because we have the same wave functions for all quarks and antiquarks, the difference being only in the normalization. How to deal with the difference between the interactions of u and d quarks of the nucleon in an effective way was shown in the previous subsection, considering a quark mass shift.

3.3 Quark substructure

The quarks in our model are effective degrees of freedom that can have substructure. The structure function of the constituent quark/antiquark can be extracted from the pion structure function, $P(x)$, with the assumption that it is dominated by the asymptotic behavior. For a massless pion, the asymptotic part of the light-front wave function implies a constant probability for the valence quark to have a given momentum fraction [58]. The pion structure function can be written as

$$v^\pi(x, Q^2) = \int_x^1 \frac{\mathrm{d}y}{y}P(y, Q^2)F^\pi_{q\bar{q}}\left(\frac{x}{y}\right), \quad (29)$$

where $F^{\pi}_{q\bar{q}}(x)$ is the pion structure function for constituent quarks from the valence wave function [58]). Assuming $F^{\pi}_{q\bar{q}}(x) = 1$ for the asymptotic form of the valence wave function,

$$v^{\pi}(x, Q^2) = \int_x^1 \frac{\mathrm{d}y}{y} P(y, Q^2)\,, \tag{30}$$

and taking the derivative over x, one gets

$$P(x, Q^2) = -x \frac{\partial}{\partial x} v^{\pi}(x, Q^2)\,, \tag{31}$$

the constituent quark/antiquark structure function.

In order to analyze how this substructure of the constituent quark can affect the structure function, in the following we consider the parametrization for $v^{\pi}(x, Q^2)$ given in [59]. The structure function of a valence quark in the pion is given by

$$x v^{\pi}(x, Q^2) \equiv x v^{\pi}(x) = N_{\pi} x^a \left(1 + A\sqrt{x} + Bx\right)(1-x)^D\,, \tag{32}$$

where the parameters are

$$\begin{aligned} N_{\pi} &= 1.212 + 0.498s + 0.009s^2\,, \\ a &= 0.517 - 0.020s\,, \\ A &= -0.037 - 0.578s\,, \\ B &= 0.241 + 0.251s\,, \\ D &= 0.383 + 0.624s\,, \\ s &= \ln \frac{\ln(Q^2/0.204^2)}{\ln(\mu^2/0.204^2)}\,. \end{aligned} \tag{33}$$

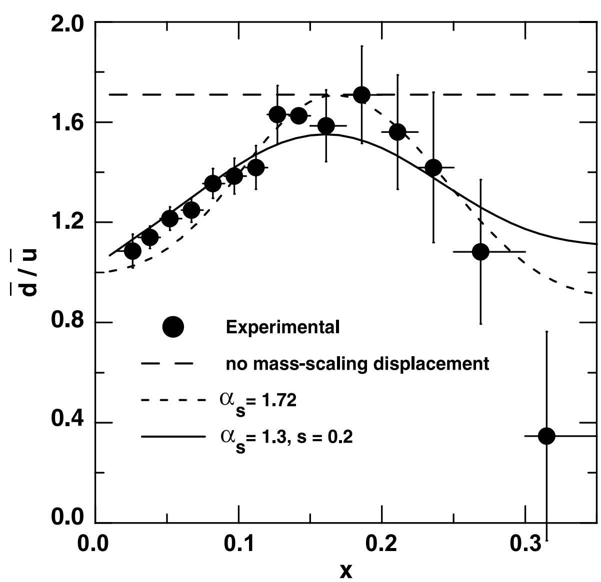

Fig. 3. The model results for the antiquark ratio $\bar{d}/\bar{u}$, as a function of x, are compared with data results obtained from [1, 2]. Without mass-scaling displacement, we obtain the constant *long-dashed line*. With the *small-dashed line curve*, we present the results with $\alpha_s = 1.72$; and, with *solid line*, the results with $\alpha_\mathrm{s} = 1.3$ and $s = 0.2$

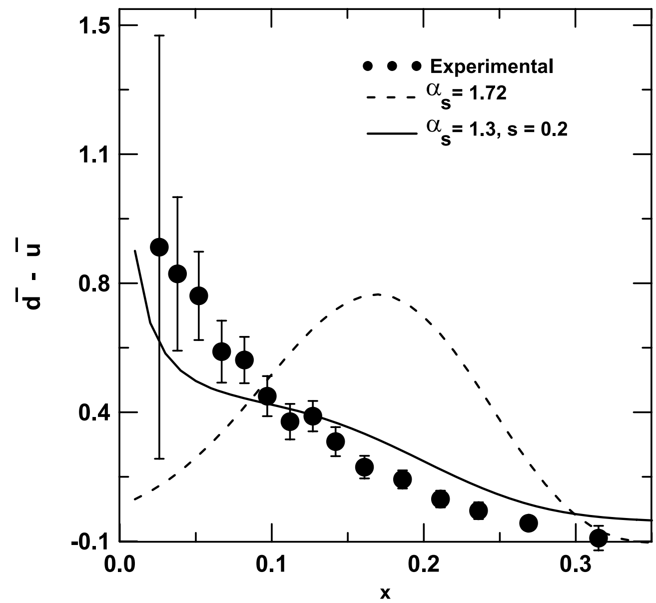

Fig. 4. Results for the difference $\bar{d} - \bar{u}$, as functions of x. The model results are compared with data from [1, 2], scaled to fixed $Q^2 = 54\,\mathrm{GeV}^2/c^2$. With the *dashed line* we have indicated the results with $\alpha_\mathrm{s} = 1.72$; and, with the *solid line*, $\alpha_\mathrm{s} = 1.3$ and $s = 0.2$

Using the above, the antiquark $\bar{q}(x)$ structure function in the nucleon from the constituent substructure is given by

$$\bar{q}_{\mathrm{const}}(x) = -\int_x^1 \frac{\partial}{\partial z} v^{\pi}(z, Q^2)\bigg|_{z=x/y} \bar{q}(y)\,\mathrm{d}y\,, \tag{34}$$

where $\bar{q}(y)$ is the quark structure function given by the model.

As we can see in the following, such an effect is relevant for obtaining a good fitting for $\bar{d} - \bar{u}$. In this way, to obtain a better fit, we need to combine the values of α_s (from the gluon splitting process) with the values of the parameter s. Without considering such a substructure, the difference $\bar{d} - \bar{u}$ presents a considerable deviation when compared with the experimental results (see Fig. 4). The correction to this problem is done by considering the substructure of the antiquarks as derived from the pion structure function, using the parametrization given in [59].

We should observe that, from construction, the constituent quark structure function should include all possible gluonic splitting processes. Therefore, a decrease is expected in the value of α_s with respect to the case in which no constituent quark substructure effects are considered in the fitting procedure. Indeed, such an expectation is verified in the results plotted in Figs. 3 and 4.

4 Main results

Once the parameters of the model are fixed to observables as the chemical potentials and the Gottfried sum rule, in order to fit the experimental data we also consider the following three free parameters: the quark mass ratio (M_u/M_q), which gives the mass scale shift; α_s, for the gluon splitting; and s, in the case that we consider pionic processes as described in the previous section.

For the first parameter we use $(M_u/M_q) = 1.25$, shifting the maximum value of the function $q(x)$ in Fig. 1, from the original 0.2 to 0.25. In Fig. 2, we show the different contributions to the ratio $\bar{d}/\bar{u}$. Without rescaling, with the dotted line we have the result of the statistical model, and, with the dot-dashed line, only the gluon contribution. In both cases, the ratio is constant. The ratio is always equal to 1 for the gluon contribution. With the dashed line we show the resulting effect of two contributions: from the statistical model and from gluonic effects ($\alpha_s = 1.72$). The solid line presents the rescaled result for the ratio, without gluon contributions.

In Figs. 3 and 4, we have two important results of the model, related to the antiquark distribution in the nucleon. In Fig. 3, we show the antiquark ratio $\bar{d}/\bar{u}$ and, in Fig. 4, the antiquark difference $\bar{d}-\bar{u}$. The initial result of the statistical model, with no shift of the distributions and without quark pair contributions, is shown in Fig. 3 by the long-dashed constant line. The experimental data, shown in Figs. 3 and 4, are from [1,2], obtained with $Q^2 = 7.35\,\mathrm{GeV}^2$. As shown in Fig. 3, the best choice for the ratio is obtained with $\alpha_s = 1.72$, which implies $\Lambda_{\mathrm{QCD}} = 0.511$ GeV. This value is considered in the calculation of the gluon contributions for the quark ratio distribution d/u, shown in Fig. 5, and also in the neutron to proton ratio distribution, F_2^n/F_2^p, shown in Fig. 6, where $Q^2 = 12\,\mathrm{GeV}^2$. With the solid line we show in Figs. 3 and 4 the results obtained by considering all the effects: the statistical model,

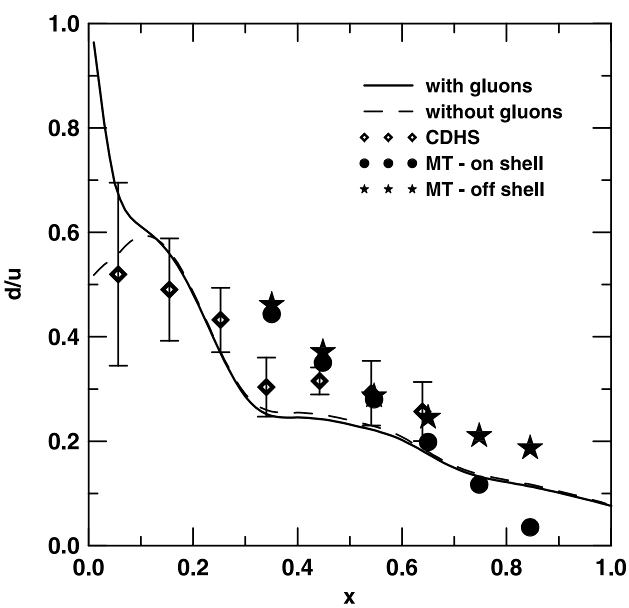

Fig. 5. Quark-ratio d/u distribution inside the proton as a function of x. The model results consider the mass-scaling displacement; without gluon splitting (*dashed line*) and with gluon splitting (*solid line*). The model is compared with experimental data (CDHS) [40] and with calculations on-shell (*solid circles*) and off-shell (*stars*) from [23], considering data from [20, 39]

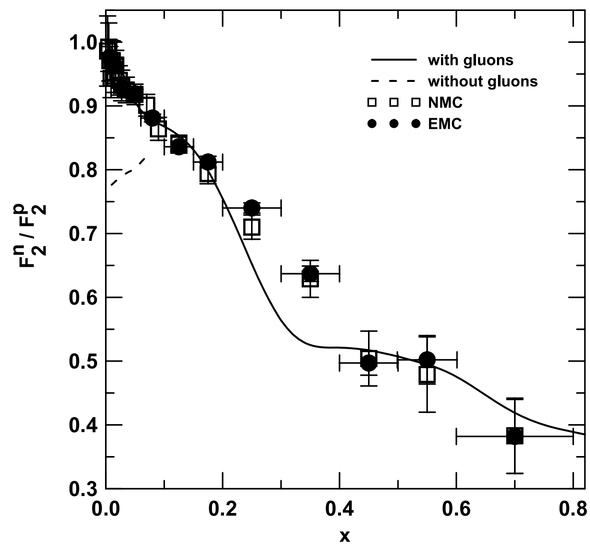

Fig. 6. The ratio F_2^n/F_2^p of the neutron to proton structure function is shown as a function of x. As in Fig. 5, the model results consider the mass shift rescaling; without gluon splitting (*dashed line*) and with gluon splitting (*solid line*). The model is compared with data from NMC [47, 48] (with Q^2 from 0.4 to $10.8\,\mathrm{GeV}^2$) and from EMC [24] (with $Q^2 = 4\,\mathrm{GeV}^2$)

mass shift, gluon splitting, and the contribution from the constituent quark substructure included through the convolution given by (34).

We observe in Fig. 4 that both, combined effects from gluon splitting and from the constituent quark substructure are relevant for the best fitting of the difference $\bar{d}-\bar{u}$. The probability effect of gluon emission decreases when the quark substructure is considered, corresponding to a variation of α_s from 1.72 to 1.3. As the constituent quark structure function should include all gluonic splitting processes, in the fitting we are forced to diminish α_s. However, one may wonder why it should be nonzero. We can raise at least three points for that:

i) the simplified assumption to extract the constituent quark structure function using the asymptotic form of the pion wave function;
ii) the quark sea within the constituent quark may be affected by the different valence content in the pion and in the nucleon wave function, and
iii) the inaccuracy in the description of the nucleon quark source by the statistical model.

Despite the simplified picture of our model, the physical ingredients, i.e., the constituent quark structure and gluon splitting process conspire to produce a somewhat consistent effect with respect to the quark sea.

As also shown in Figs. 5 and 6, respectively, for the ratios d/u and F_2^n/F_2^p, the model provides good fits to the available experimental data, with gluonic contributions affecting mainly the low-x region of such ratios. These results are consistent with the ones presented in Fig. 3, from which we have verified that, in order to fit the ratios, the inclusion of the constituent quark substructure beyond the gluon splitting process is not so relevant.

As an additional remark, for the d/u results given in Fig. 5, we note that two different ways were considered in [23] to extract the values from the experimental data given in [20, 39]: on-shell and off-shell, with the off-shell values obtained considering nuclear effects [23]. The results of our model, as shown for x larger than ~ 0.6, follow a trend that approaches the off-shell results, when increasing x.

5 Conclusion and discussion

In a statistical quark model in which the quark energy levels are given by a central confining potential, we obtain results for the light sea-quark asymmetry, $\bar{d}/\bar{u}$ and also for the ratio d/u. The model is parameterized by the corresponding experimental data. The sea-quark contribution is composed of two parts: the statistical model adjusts the Gottfried sum rule violation and the flavor normalization inside the nucleon, and the gluon splitting processes which give equal sea components. As we have used the same confining potential in the statistical model, we obtain a constant ratio between the structure functions, in spite of the fact that we fit the GSR violation with this model.

The qualitative difference between the structure functions comes from the fact that the light quarks with different flavors (u and d and the corresponding antiparticles) have different energies. The source of the degeneracy lifting is given by instanton induced interactions between the quarks. A simple mathematical trick, based on the Dirac delta distribution, was used to obtain the shift of the given structure functions (which are equal a priori), producing a quite good fit to the $d(x)/u(x)$ and $\bar{d}(x)/\bar{u}(x)$ ratios in the proton.

The constituent quark structure function in our model should include all possible gluonic splitting processes, from construction. Indeed, we observed that the probability of gluon emission decreases when we consider the quark substructure (see Sect. 3.3 and Figs. 3 and 4). We understand that a non-vanishing gluon splitting contribution is necessary to compensate in part for the simplified assumptions of the nucleon and pion wave functions. In particular, we have used the asymptotic form of the pion wave function to extract the constituent quark structure function and assumed that it is unchanged within the nucleon. So it is reasonable to think that by considering more realistic pion and nucleon wave functions, one can diminish further the importance of explicit gluon contributions in the model.

Finally, we note that, even considering measurement processes for the $\bar{d}/\bar{u}$ and d/u to be different, our phenomenological considerations are quite good, with our numerical results approaching both experimental data (see Figs. 3–6). In other words, the statistical quark model, the difference between the confining potentials for the u and d quarks in the nucleon (due to instanton induced interactions), and the contributions from the gluon splitting process are all relevant to the fit to the data. Eventually, to further improve the model, some other features may be considered, perhaps a pion cloud or the binding effects of the EMC, since our results approach the off results of [23] for increasing values of x.

Acknowledgements. We thank Fundação de Amparo à Pesquisa do Estado de São Paulo (FAPESP) and Conselho Nacional de Desenvolvimento Cientí fico e Tecnológico (CNPq) for partial support.

References

1. J.C. Peng et al., Phys. Rev. D **58**, 092 004 (1998)
2. E.A. Hawker et al., Phys. Rev. Lett. **80**, 3715 (1998)
3. K. Gottfried, Phys. Rev. Lett. **18**, 1174 (1967)
4. F. Carvalho, F.O. Durães, F.S. Navarra, M. Nielsen, Phys. Rev. D **60**, 094 015 (1999)
5. M. Alberg, E.M. Henley, Nucl. Phys. A **663**, 301 (2000)
6. E.J. Eichten, I. Innchliffe, C. Quigg, Phys. Rev. D **45**, 2269 (1992)
7. E.M. Henley, G.A. Miller, Phys. Lett. B **251**, 453 (1990)
8. S. Kumano, Phys. Rev. D **43**, 59 (1991)
9. S. Kumano, Phys. Rev. D **43**, 3067 (1991)
10. A.I. Signal, A.W. Schreiber, A.W. Thomas, Mod. Phys. Lett. A **6**, 271 (1991)
11. H. Holtmann, A. Szczurek, J. Speth, Nucl. Phys. A **569**, 631 (1996)
12. S. Kumano, Phys. Rep. **303**, 183 (1998)
13. G.T. Garvey, J.-C. Peng, Prog. Part. Nucl. Phys. **47**, 203 (2001)
14. R.D. Field, R.P. Feynman, Phys. Rev. D **15**, 2590 (1977)
15. C. Bourrely, F. Buccella, J. Soffer, Eur. Phys. J. C **23**, 487 (2002)
16. C. Bourrely, F. Buccella, J. Soffer, Eur. Phys. J. C **41**, 327 (2005)
17. J. Cleymans, R.L. Thews, Z. Phys. C **37**, 315 (1988)
18. E. Mac, E. Ugaz, Z. Phys. C **43**, 655 (1989)
19. L.A. Trevisan, T. Frederico, L. Tomio, Eur. Phys. J. C **11**, 351 (1999)
20. L.W. Whitlow et al., Phys. Lett. B **282**, 475 (1992)
21. L.L. Frankfurt, M.I. Strikman, Phys. Rep. **160**, 235 (1988)
22. S. Liuti, F. Gross, Phys. Lett. B **356**, 157 (1995)
23. W. Melnitchouk, A.W. Thomas, Phys. Lett. B **377**, 11 (1996)
24. European Muon Collaboration, J.J. Aubert et al., Nucl. Phys. B **293**, 740 (1987)
25. W. Melnitchouk, J. Speth, A.W. Thomas, Phys. Lett. B **435**, 420 (1998)
26. P. Souder, in: Proceedings of the workshop on CEBAF at Higher Energies CEBAF, Newport News, 1994
27. R. Michaels, in: Physics and Instrumentation with 6–12 GeV Beams, Jefferson Lab, p. 347 (1998)
28. I.R. Afnan et al., Phys. Rev. C **68**, 035 201 (2003)
29. R.P. Feynman, Photon Hadron Interactions (Benjamin, Reading, Massachusetts, 1972)
30. F.E. Close, A.W. Thomas, Phys. Lett. B **212**, 227 (1988)
31. W. Melnitchouk, Phys. Rev. Lett. **86**, 35 (2001)
32. L.A. Trevisan, L. Tomio, Nucl. Phys. A **689**, 485c (2001)
33. E. Eichten, I. Hinchliffe, K. Lane, C. Quigg, Rev. Mod. Phys. **56**, 579 (1984)
34. M. Diemoz et al., Z. Phys. C **39**, 21 (1988)
35. A.D. Martin, R. Roberts, W.J. Stirling, Phys. Rev. D **50**, 6734 (1994)

36. CTEQ Collaboration, H.L. Lai et al., Phys. Rev. D **51**, 4763 (1995)
37. G.R. Farrar, D.R. Jackson, Phys. Rev. Lett. **35**, 1416 (1975)
38. S.J. Brodsky, M. Burkardt, I. Schmidt, Nucl. Phys. B **441**, 197 (1995)
39. J. Gomez et al., Phys. Rev. D **49**, 4348 (1994)
40. H. Abramowicz et al., Z. Phys. C **25**, 29 (1983)
41. P.L. Ferreira, J.A. Helayel, N. Zagury, Nuovo Cim. A **55**, 215 (1980)
42. A.I. Signal, A.W. Thomas, Phys. Rev. D **40**, 2832 (1989)
43. H. Weigel, Phys. Rev. D **55**, 6910 (1997)
44. M. Wakamatsu, Phys. Rev. D **67**, 034 005 (2003)
45. H. Dahiya, M. Gupta, Eur. Phys. J. C **52**, 571 (2007)
46. J. Alwall, G. Ingelman, Phys. Rev. D **71**, 094 015 (2005)
47. P. Amaudruz et al., Phys. Rev. Lett. **66**, 2712 (1991)
48. M. Arneodo et al., Phys. Rev. D **50**, R1 (1994)
49. F. Olness et al., Eur. Phys. J. C **40**, 145 (2005)
50. C. Bourrely, J. Soffer, F. Buccella, Phys. Lett. B **648**, 39 (2007)
51. R.G. Roberts, The Structure of the Proton – Deep Inelastic Scattering (Cambridge University Press, Cambridge, 1990)
52. A.O. Bazarko et al., Z. Phys. C **65**, 189 (1995)
53. A.E. Dorokhov, N.I. Kochelev, Y.A. Zubov, Sov. J. Part. Nucl. **23**, 522 (1992)
54. F. Halzen, A.D. Martin, Quarks and Leptons – An Introductory Course in Modern Particle Physics (Wiley, New York, 1984), p. 215
55. G. Altarelli, G. Parisi, Nucl. Phys. B **126**, 298 (1977)
56. H.R. Christiansen, J. Magnin, Phys. Lett. B **445**, 8 (1998)
57. J. Magnin, H.R. Christiansen, Phys. Rev. D **61**, 054 006 (2000)
58. T. Frederico, G. Miller, Phys. Rev. D **50**, 210 (1994)
59. M. Glück, E. Reya, I. Schiebein, Eur. Phys. J. C **10**, 313 (1999)